Supplementary Information

Copper Peroxide Nanodots Decorated Gold Nanostar/Silica Nanorod Janus Nanostructure with NIR-II Photothermal and Acid-Triggered Hydroxyl Radicals Generation Properties for Effective Treatment on Wound Infection

Yan Lu[1], Rui Xu[1], Wei Liu[1], Xiling Song, Wanqin Cai, Yuan Fang, Wei Xue, Siming Yu**

Key Laboratory of Biomaterials of Guangdong Higher Education Institutes, Department of Biomedical Engineering, Jinan University, Guangzhou 510632, China

[1] Authors contributed equally to this work.

*Corresponding authors: Siming Yu (siming_yu@hotmail.com), Wei Xue (weixue_jnu@hotmail.com).

Figure S1. TEM images of SiNR (A), Au NPs/SiNR (B) and GNS/SiNR (C).

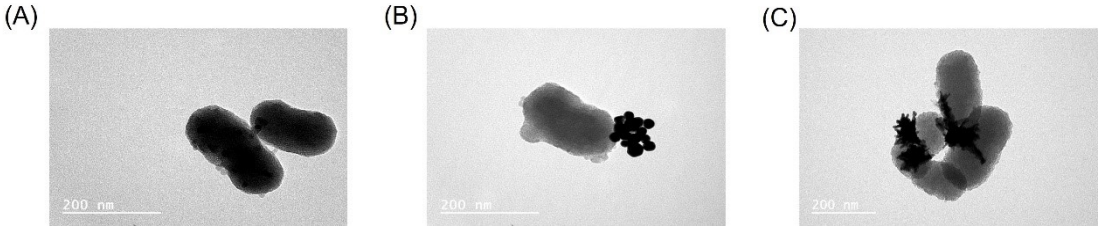

Figure S2. Intensity-weighted size distribution of SiNR (A) and GNS/SiNR (B).

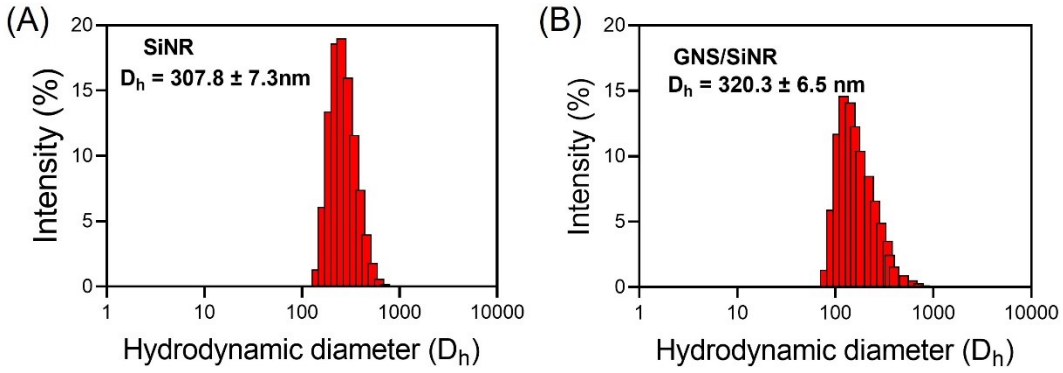

Figure S3. XRD spectrum of GNS@CP/SiNR.

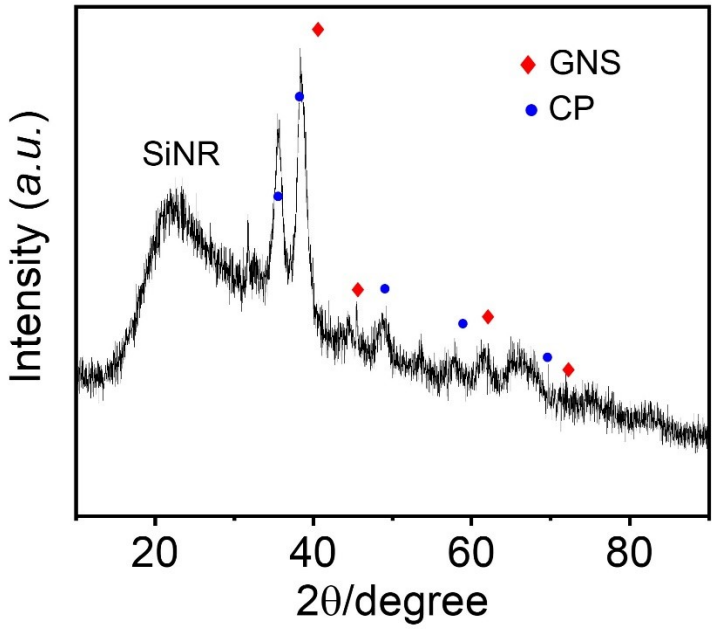

Figure S4. Changes in D_h and Zeta potential of GNS@CP/SiNR dispersion over a period of 48 h.

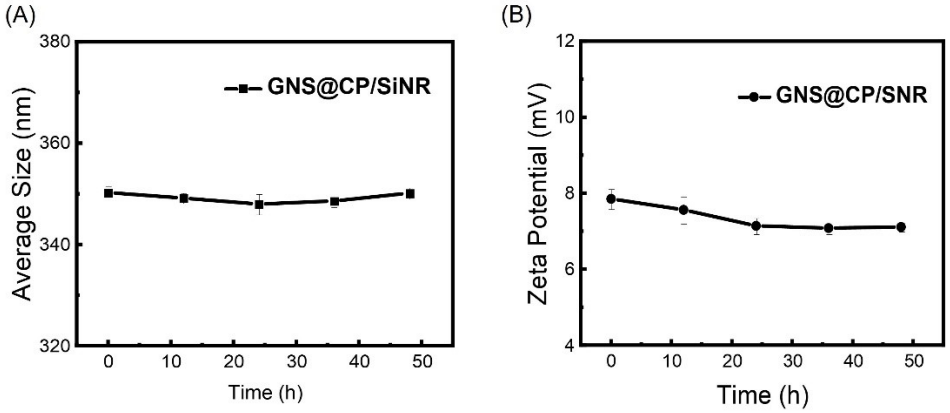

Figure S5. (A) Cu^{2+} release profiles of GNS@CP/SiNR exposed in different pH conditions. (B) Comparison of the Cu^{2+} release rate in different pH conditions after 30 min incubation.

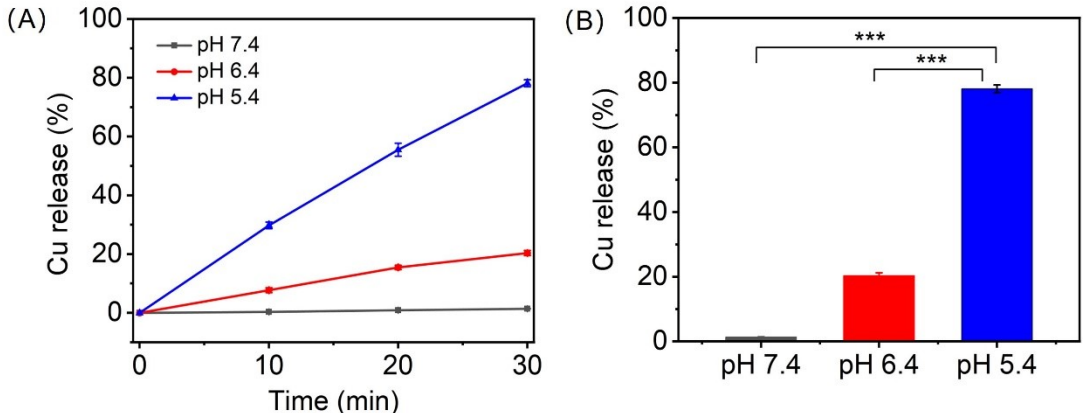

Figure S6. Color changes of $KMnO_4$ solution with addition of 10-30 mM H_2O_2 and GNS@CP/SiNR with different concentrations.

Figure S7. (A) H_2O_2 release profiles of GNS@CP/SiNR exposed in different pH conditions. (B) Comparison of the H_2O_2 release rate in different pH conditions after 30 min incubation.

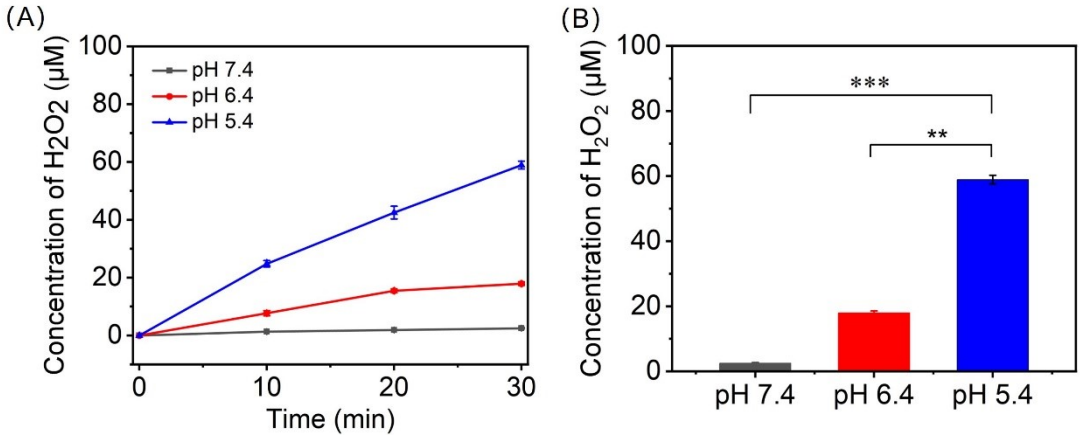

Figure S8. (A) UV-Vis spectra of TMB solutions treated with GNS@CP/SiNR of different concentrations in pH 6.4 condition. (B) Digital image shows the TMB color changes in different concentrations.

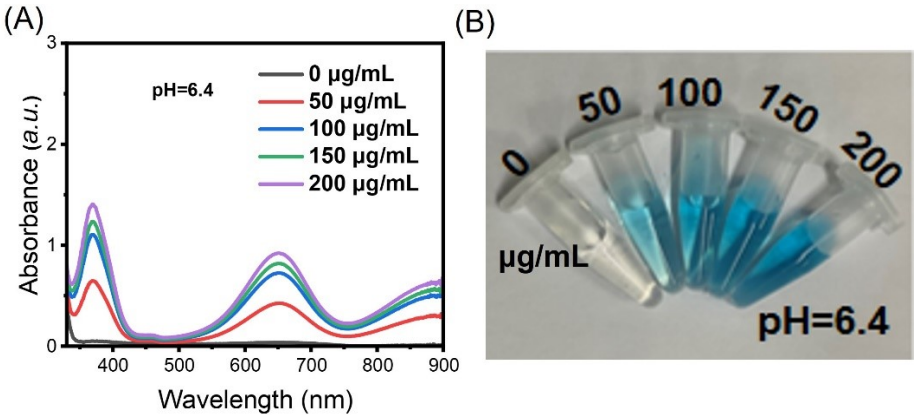

Figure S9. (A) UV-Vis spectra of TMB solutions treated with GNS@CP/SiNR of different concentrations in pH 7.4 condition. (B) Digital image shows the TMB color changes in different concentrations.

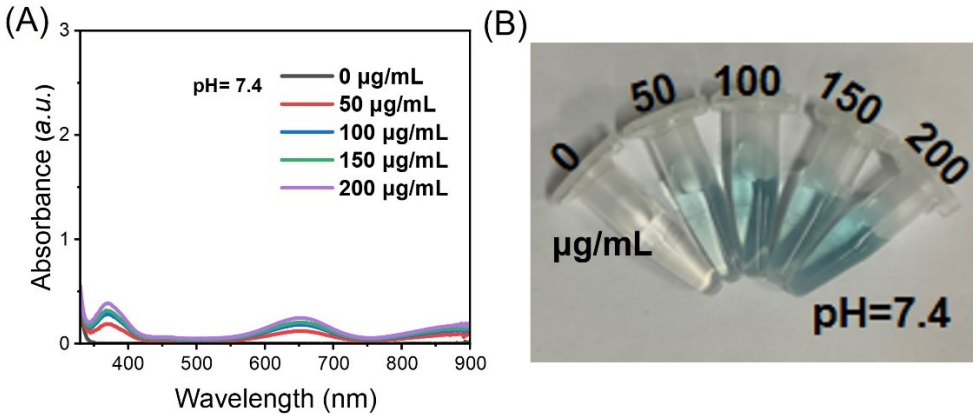

Figure S10. Histogram showing the antibacterial efficiency of different treatments against *E. coli*.

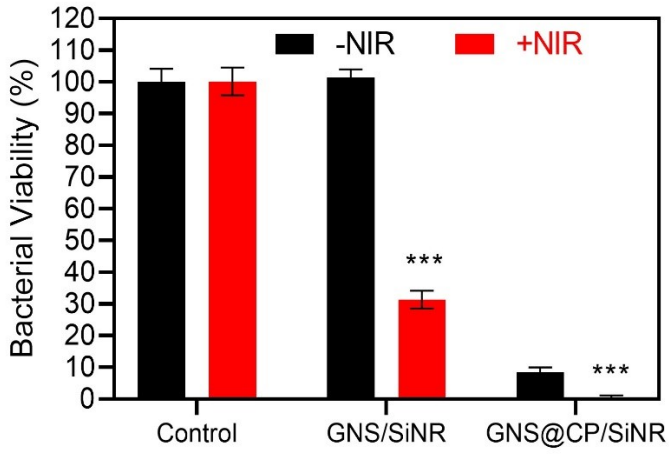

Figure S11. (A) Crystalline violet stained *E. coli* after different treatments and the corresponding OD_{570} values (B). (C) Crystalline violet stained *E. coli* underwent GNS@CP/SiNR + NIR treatment with different concentrations and the corresponding OD_{570} values (D).

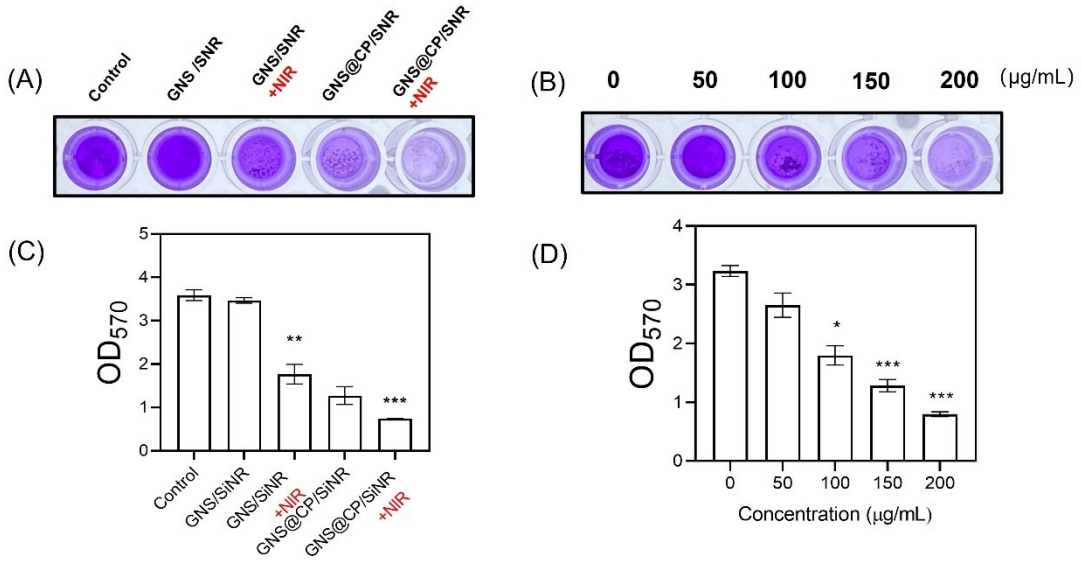

Figure S12. (A) CLSM images of *E. coli* biofilm stained with SYTO-9/PI dual fluorescent dyes after different treatments and the corresponding histogram showing the percentage of live/dead bacteria (B). Scale bar represents 20 μm.

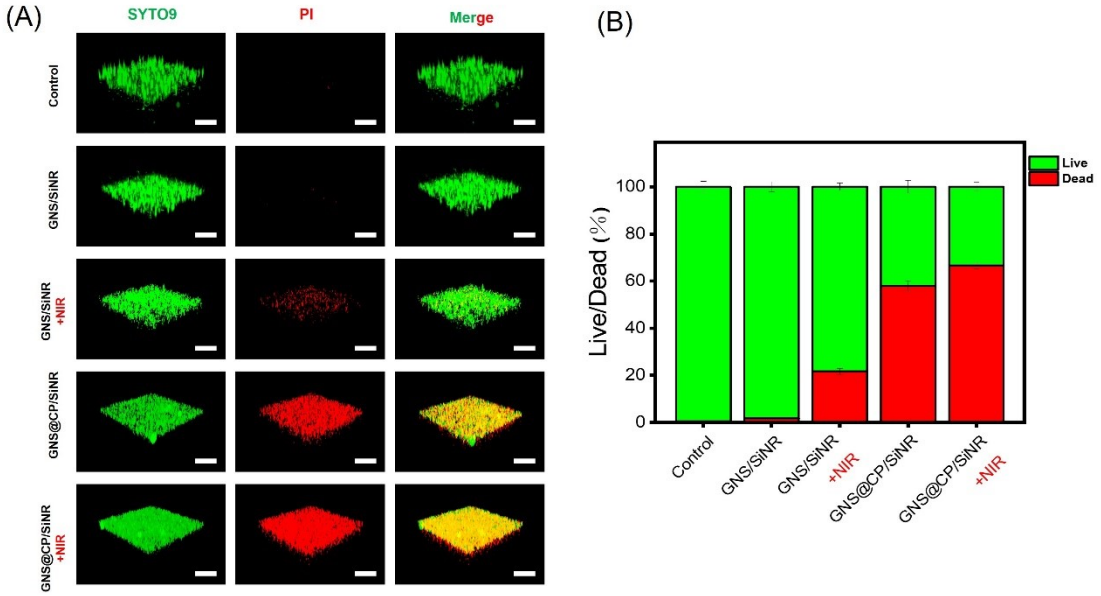

Figure S13. Histogram shows the percentage of live/dead *E. coli* (A) and *S. aureus* (B) underwent different treatments.

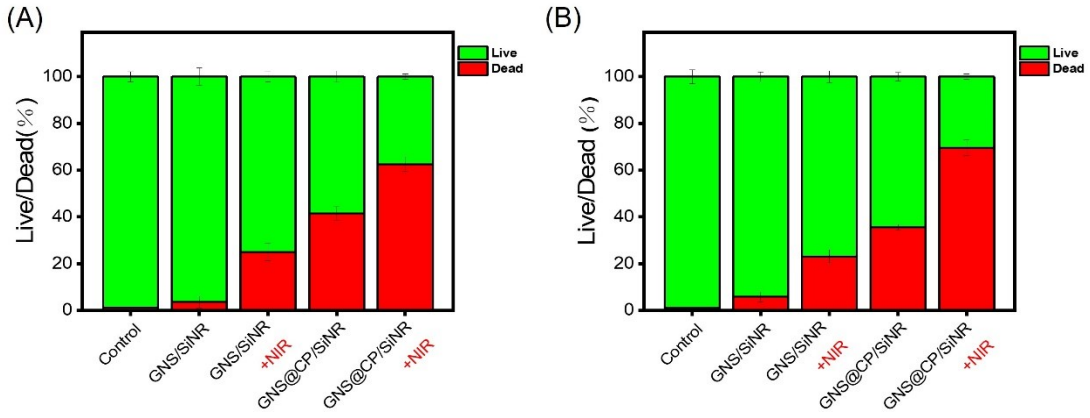

Figure S14. CLSM images of *E. coli* stained by DCFH-DA fluorescent dye showing the intracellular ROS level in treated groups of Control, GNS/SiNR, GNS/SiNR + NIR and GNS@CP/SiNR.

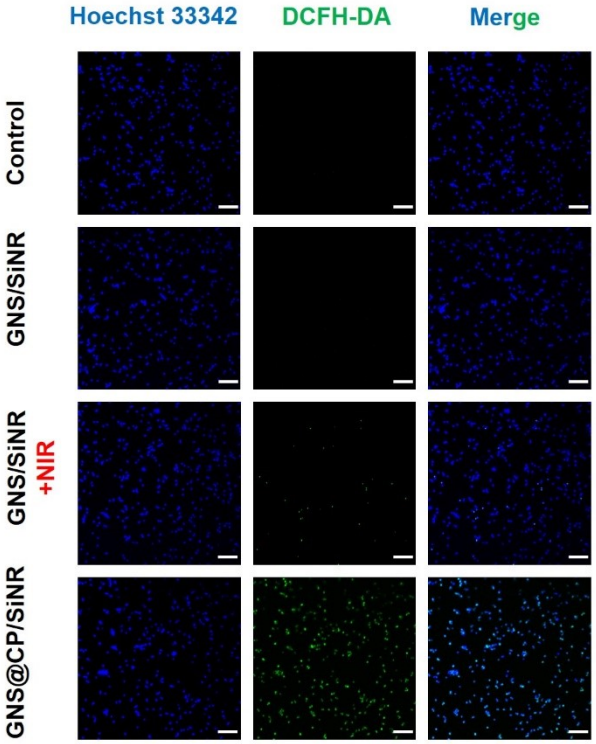

Figure S15. CLSM images of *S. aureus* stained by DCFH-DA fluorescent dye showing the intracellular ROS level in treated groups of Control, GNS/SiNR, GNS/SiNR + NIR and GNS@CP/SiNR.

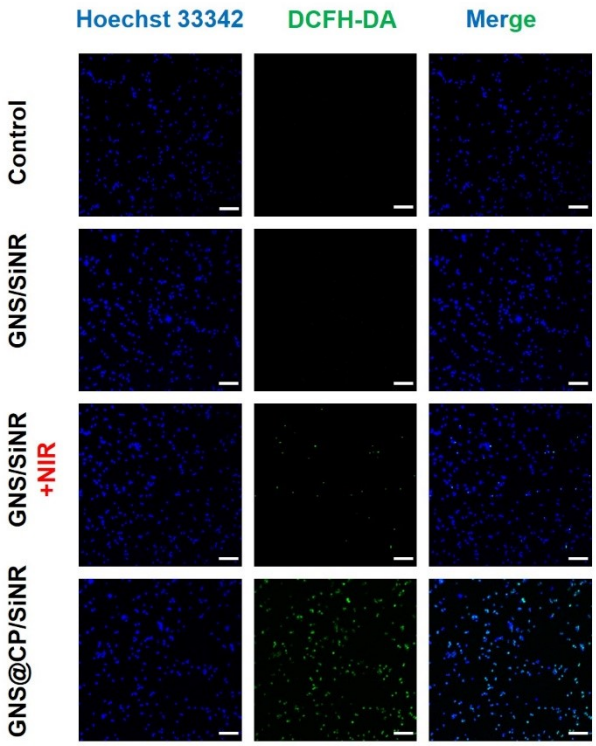

Figure S16. (A) CLSM images of *E. coli* stained by ThiolTrace Violet 500 fluorescent probe after different treatments and the corresponding mean fluorescent intensity (B). Scale bar represents 10 μm.

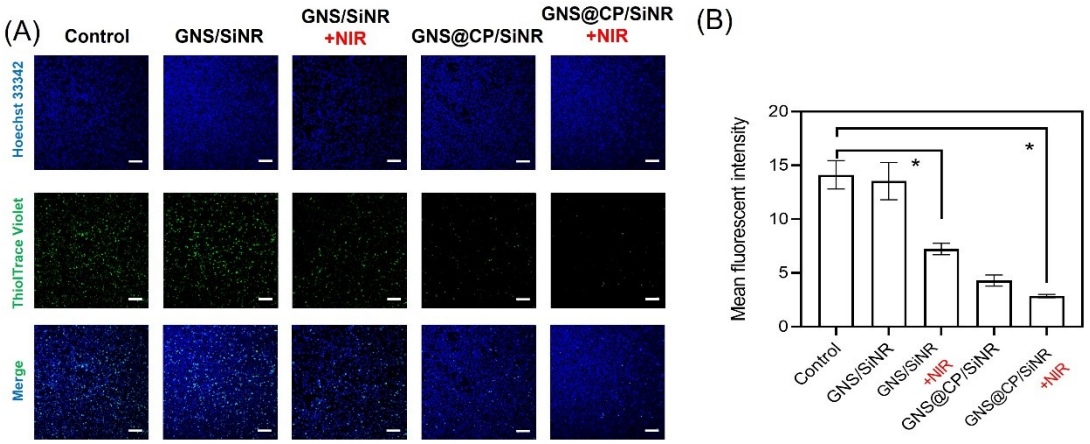

Figure S17. (A) CLSM images of TUNEL stained *E. coli* after different treatments and the corresponding mean fluorescent intensity (B). Scale bar represents 10 μm.

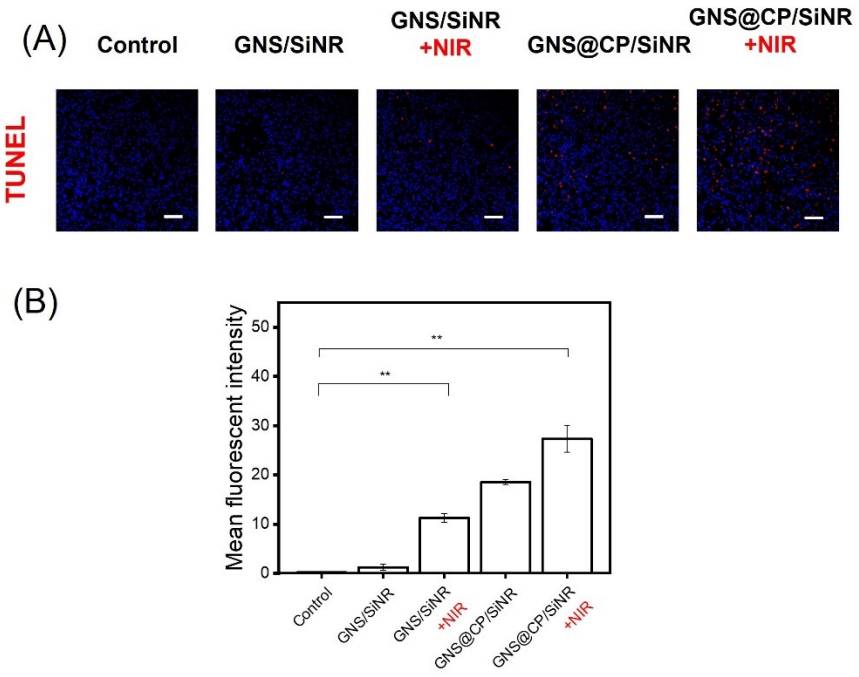

Figure S18. Agar plates showing the remanent bacterial colonies in different treated groups in different days.

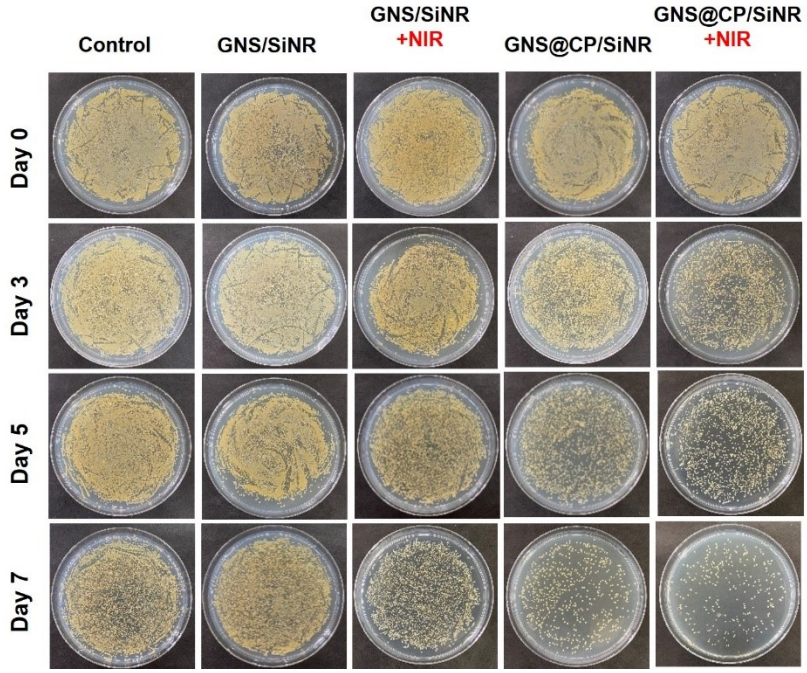

Figure S19. Cell viability of NIH/3T3 cells underwent treatments of GNS/SiNR and GNS@CP/SiNR with different concentrations.

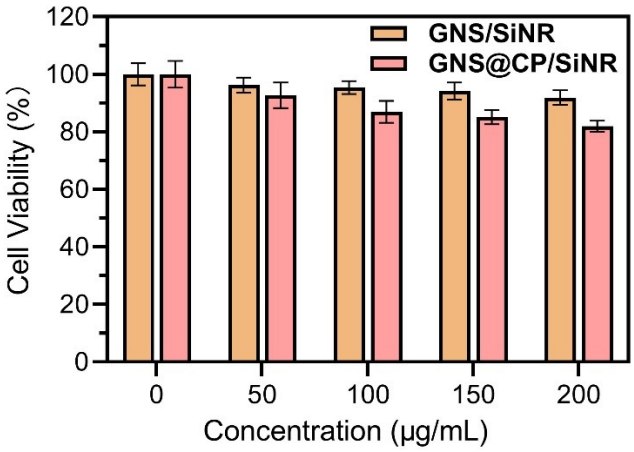

Figure S20. H&E histological images of rat's heart, liver, spleen, lung and kidney after 10 days of different treatments. Scale bar represents 100 μm.

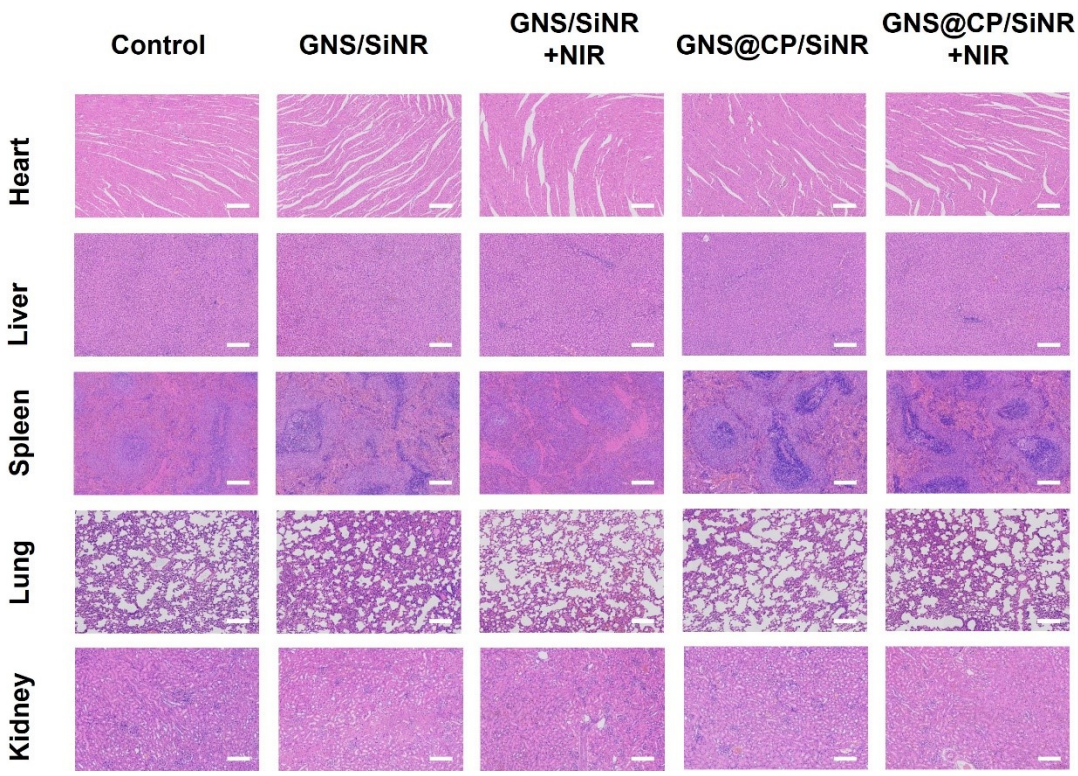

Figure S21. Blood biochemical indicators of rats under 10 days of different treatments.

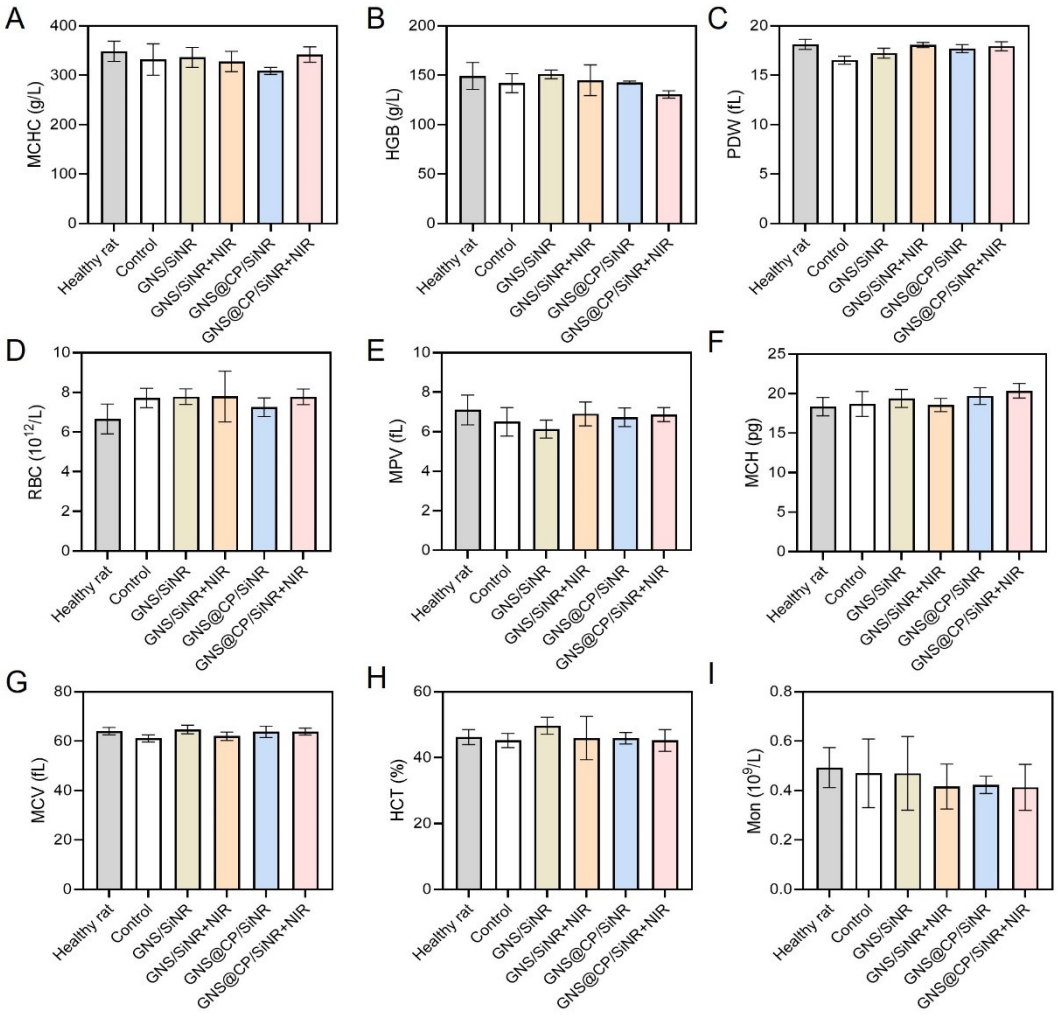

Figure S22. Changes in rats' weight in different treated groups during the whole treated period.